Biochemical and functional evaluation of the dystrophin carboxy-terminal domain for micro-dystrophin gene therapy in cardiac and skeletal muscles in the DMD^{mdx} rat model

A. Bourdon[1*], V. François[1], L. Zhang[2], A. Lafoux[3], B. Fraysse[1], G. Toumaniantz[4], T. Larcher[5], T. Girard[1], M. Ledevin[5], C. Lebreton[1], A. Hivonnait[4], A. Creismeas[1], M. Allais[1], J. Guguin[1], V. Blouin[1], S. Remy[6], I. Anegon[6], C. Huchet[1,3], P. Moullier[1,7], G. Dickson[8], L. Popplewell[8], O. Adjali[1], F. Montanaro[9], C. Le Guiner[1*]

[1]Translational Gene Therapy Laboratory, Université de Nantes, INSERM UMR 1089, CHU de Nantes, France, [2] Mass Spectrometry and Proteomics Facility, the Ohio State University, Columbus, USA, [3]Therassay platform, Capacités, Université de Nantes, France, [4]L'Institut du Thorax, Université de Nantes, CNRS, INSERM UMR 1087, France, [5]INRAE, Oniris, PAnTher, APEX, Nantes, France, [6]Center for Research in Transplantation and Immunology, INSERM UMR 1064, Nantes, France, [7]Asklepios BioPharmaceutical, North Carolina, USA, [8]Royal Holloway, University of London, United Kingdom, [9]UCL Great Ormond Street Institute of Child Health, London, United Kingdom

*Contact: audrey.bourdon@univ-nantes.fr, caroline.le-guiner@univ-nantes.fr

Introduction

Duchenne Muscular Dystrophy (DMD) is a muscle wasting disorder caused by mutations in the gene encoding dystrophin, a protein essential for the integrity of muscular fibers. Gene therapy using micro-dystrophin (MD) transgenes and recombinant adeno-associated virus (rAAV) vectors is one of the most promising therapeutic approaches for DMD. Three MDs are currently evaluated in patients. Due to the limited packaging capacity of rAAV vectors (5kb), the choice was done to not include dystrophin C-terminal (CT) domain in these MDs. Yet, this domain is known to recruit α1- and β1-syntrophins and α-dystrobrevin, major members of the dystrophin associated protein complex (DAPC), which act as signaling and structural mediator of muscle cells.

In this study, we explored the impact of inclusion of the CT in one of these MDs, called MD1, in the DMD^{mdx} rat, a new animal model of DMD, which mimics the clinical pathology at both the muscular and cardiac levels. We evaluated if the inclusion of the dystrophin CT domain in MD1 could improve (i) its efficacy at recovering DAPC interactions, and (ii) its therapeutic potential, in both skeletal and cardiac muscles of DMD^{mdx} rats.

Using mass spectrometry (LC-MS/MS) analysis on MD/dystrophin enriched fractions by co-immunoprecipitation (co-IP), we determined the DAPC composition of skeletal and cardiac muscles from rats expressing native dystrophine (WT rats) or MDs including progressively the dystrophin CT domain : MD1, MD2, MD3 or MD4 (rAAV-MD1, -MD2, -MD3, -MD4 injected DMD^{mdx} rats).

Then, we chose to compare the therapeutic potential of MD1 and MD3 after systemic injection of rAAV-MD1 or –MD3 at a known sub-therapeutic dose for MD1 (1E13 vg/dg), to evaluate and potentially highlight a difference in efficacy between these two products. The relevance of the DMD^{mdx} rat model allowed us to evaluate a wide range of parameters as the histological aspect, the calcium homeostasis in skeletal muscle and heart and the *in vivo* muscle strength and cardiac function.

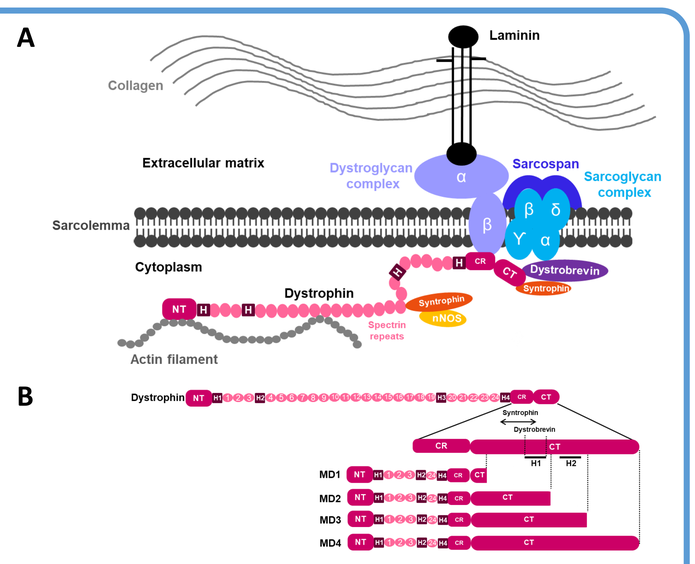

Figure 1: Schematic representations of (A) the DAPC and (B) the dystrophin protein structure (with focus on the CT domain) and of the different MD constructs evaluated in this study.

IMPACT OF THE DYSTROPHIN CT DOMAIN ON THE DAPC COMPOSITION

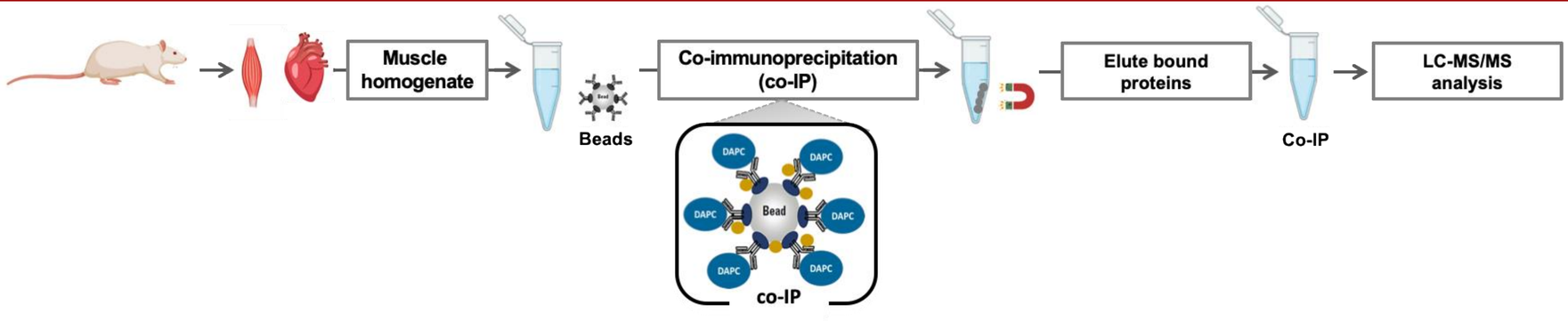

Figure 2: Experimental procedure used for the identification, by LC-MS/MS analysis, of DAPC members in co-IP samples obtained from skeletal muscles and heart of WT and rAAV2/9-MD1, -MD2, -MD3, -MD4 injected DMD^{mdx} rats.
Proteins were extracted from skeletal muscles (pectoralis or tibialis anterior) and heart. Co-immunoprecipitations of MD/dystrophin and its associated protein partners (DAPC) were performed using magnetic G-protein beads coupled to an anti-MD/dystrophin antibody (MANEX1011B). Bound proteins were eluted and processed for LC-MS/MS.

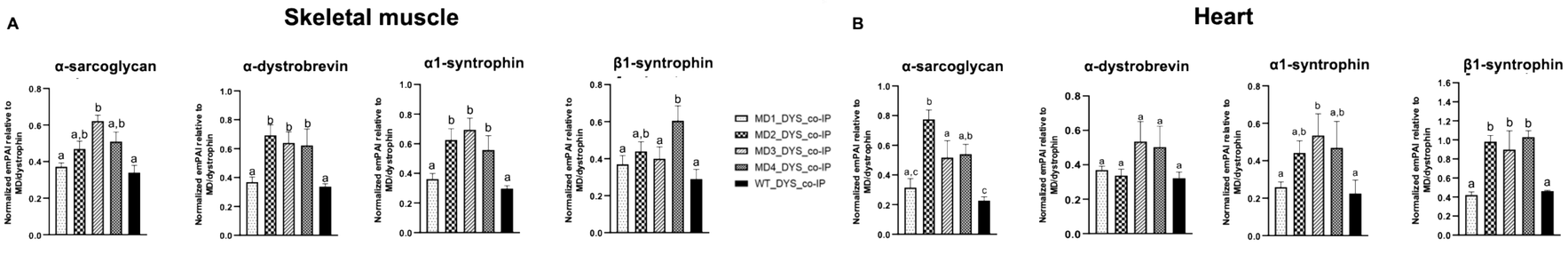

Figure 3: Comparison of DAPC proteins abundance relative to MD/dystrophin between co-IP obtained from skeletal and cardiac muscles of WT and rAAV2/9-MD1, -MD2, -MD3, -MD4 injected DMD^{mdx} rats.
Scaffold proteomic software was used for LC-MS/MS data analysis and calculation of emPAI (Exponentially Modified Protein Abundance Index) values to estimate abundance of each identified protein within the total set of identified proteins. Relative abundance to MD/dystrophin were calculated by dividing the normalized emPAI of each DAPC partner by the normalized emPAI of the MD/dystrophin expressed in the same sample. Relative abundances of α-sarcoglycan, α-dystrobrevin, α1-, β1-syntrophin in co-IP from skeletal and cardiac muscles were compared between MD1_DYS_co-IP (N=4), MD2_DYS_co-IP (N=4), MD3_DYS_co-IP (N=4), MD4_DYS_co-IP (N=4 for skeletal muscles and N=3 for heart) and WT_DYS_co-IP (N=4) experimental groups. Data are presented as mean ± SEM. Statistics were done using a 2-way ANOVA followed by a multiple comparison post-hoc "original FDR method of Benjamini and Hochberg". Q-values (corrected P-value) ≤0.05 were considered statistically significant. Values sharing the same letter are not statistically different from each other.

→ MD1 EXPRESSION IS SUFFICIENT TO RESTORE, AT A PHYSIOLOGICAL LEVEL, THE INTERACTIONS OF DAPC PARTNERS IN SKELETAL AND CARDIAC MUSCLES OF DMD^{MDX} RATS

→ INCLUSION OF THE CT DOMAIN IN MD1 INCREASES THE RECRUITMENT OF SOME DAPC PARTNERS AT SUPRA-PHYSIOLOGICAL LEVELS

IMPACT OF THE DYSTROPHIN CT DOMAIN ON THE THERAPEUTIC EFFICACY OF A MD TRANSGENE

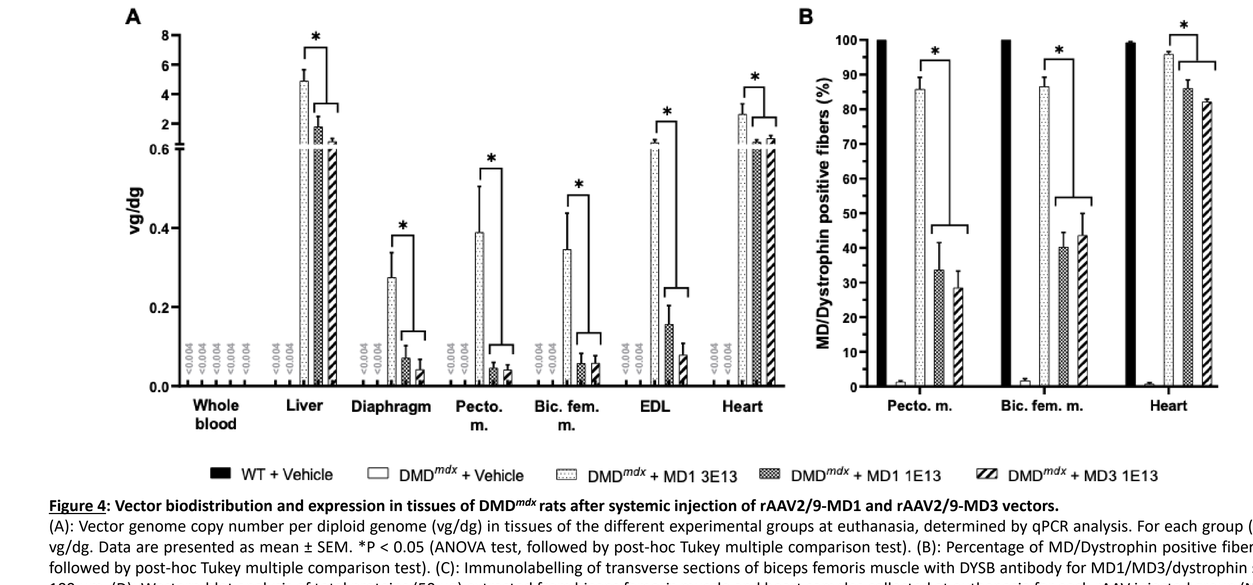

Figure 4: Vector biodistribution and expression in tissues of DMD^{mdx} rats after systemic injection of rAAV2/9-MD1 and rAAV2/9-MD3 vectors.
(A): Vector genome copy number per diploid genome (vg/dg) in tissues of the different experimental groups at euthanasia, determined by qPCR analysis. For each group (N=6 animals per group), the analysis was performed on whole blood, liver, diaphragm, heart, pectoralis, biceps femoris and EDL muscles. The limit of quantification (LOQ) was 0.004 vg/dg. Data are presented as mean ± SEM. *P < 0.05 (ANOVA test, followed by post-hoc Tukey multiple comparison test). (B): Percentage of MD/Dystrophin positive fibers determined at euthanasia by immunolabelling in heart, pectoralis and biceps femoris muscles (N=6 animals per group). Data are presented as mean ± SEM. *p<0.05 (ANOVA test, followed by post-hoc Tukey multiple comparison test). (C): Immunolabelling of transverse sections of biceps femoris muscle with DYSB antibody for MD1/MD3/dystrophin staining (green) and with WGA conjugate for connective tissue (red). Representative images corresponding to samples collected at euthanasia for each experimental group. Scale bar, 100 µm. (D): Western-blot analysis of total proteins (50 µg) extracted from biceps femoris muscle and heart samples collected at euthanasia for each rAAV injected group (N=4 animals per group). The blots were stained with MANEX-1011C to reveal the presence of the 138 kDa MD1 and the 160 kDa MD3 proteins. α-tubulin antibody as a loading control.

→ MD1 AND MD3 ARE SIMILARLY AND PROPERLY EXPRESSED IN SKELETAL MUSCLES AND HEART AFTER SYSTEMIC INJECTION IN DMD^{MDX} RATS

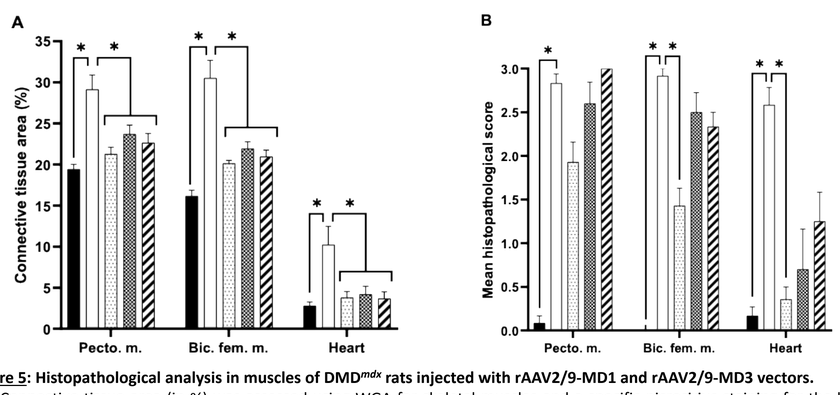

Figure 5: Histopathological analysis in muscles of DMD^{mdx} rats injected with rAAV2/9-MD1 and rAAV2/9-MD3 vectors.
(A): Connective tissue area (in %) was assessed using WGA for skeletal muscles and a specific picrosirius staining for the heart. Analysis were performed at sacrifice on heart, pectoralis and biceps femoris muscles (N=6 animals per group). Data are presented as mean ± SEM. * p<0.05 (Parametric ANOVA test, followed by post-hoc Tukey multiple comparison test). (B): Muscle histopathological score in skeletal muscles and heart samples. Muscles lesions were scored using the following system: 0 = absence of lesions, 1 = presence of some regenerative activity as evidenced by centronucleated fibers, 2 = presence of degenerated/necrotic fibers, 3 = tissue remodeling and fiber replacement by fibrosis. In the heart, scoring was based on the presence of inflammatory and fibrotic areas (1 = 1 area, 2 = multiple isolated areas, 3 = extensive/coalescing multiple areas). Analysis were performed at sacrifice on heart, pectoralis and biceps femoris muscles (N=6 animals per group). Data are presented as mean ± SEM. *p<0.05 (Nonparametric Kruskal-Wallis test, followed by a post-hoc Dunn's multiple comparison test).

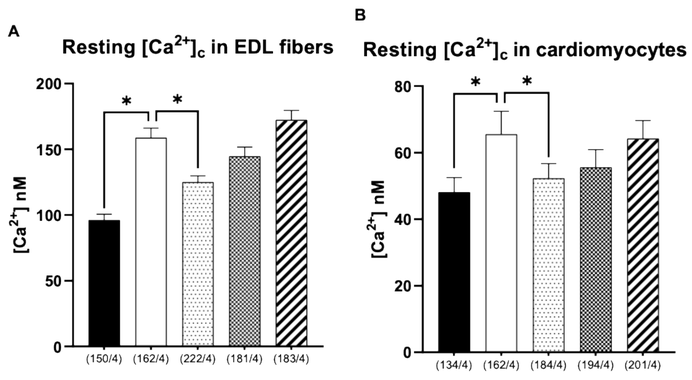

Figure 6: Analysis of calcium homeostasis in skeletal muscles and isolated cardiomyocytes of DMD^{mdx} rats injected with rAAV2/9-MD1 and rAAV2/9-MD3 vectors.
Resting intracellular-free calcium concentration ([Ca2+]c) of EDL muscle fibers (A) and isolated cardiomyocytes (B) obtained from animals from the different experimental groups. [Ca2+]c was calculated in fura-2-loaded isolated muscle fibers using calibration parameters of Grynkiewicz's equation determined in situ. A calibration was performed for each muscle used. Data are presented as mean ± SEM from n muscle fibers and N animals (n/N). *p<0.05 (ANOVA test, followed by post-hoc Bonferroni multiple comparison test).

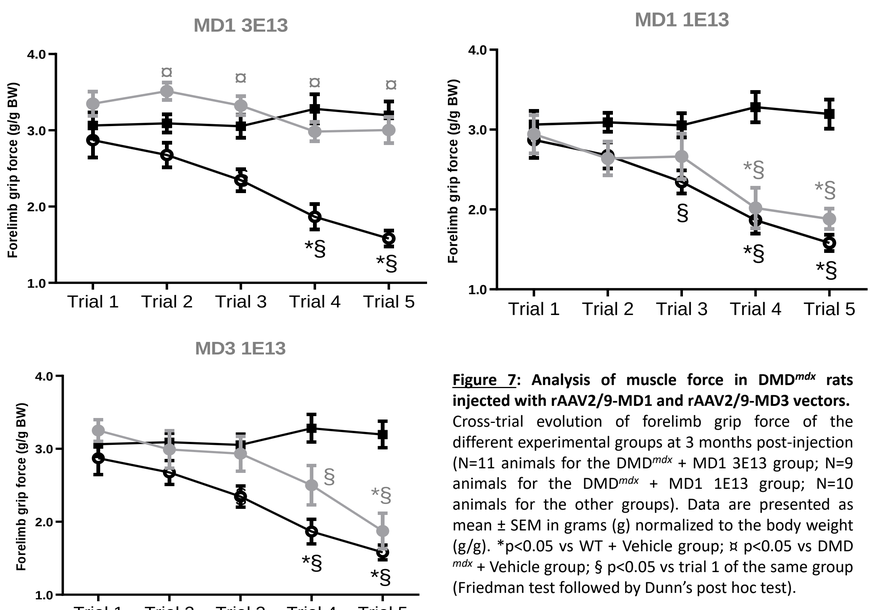

Figure 7: Analysis of muscle force in DMD^{mdx} rats injected with rAAV2/9-MD1 and rAAV2/9-MD3 vectors.
Cross-trial evolution of forelimb grip force of the different experimental groups at 3 months post-injection (N=11 animals for the DMD^{mdx} + MD1 3E13 group; N=9 animals for the DMD^{mdx} + MD1 1E13 group; N=10 animals for the other groups). Data are presented as mean ± SEM in grams (g) normalized to the body weight (g/g). *p<0.05 vs WT + Vehicle group; ¤ p<0.05 vs DMD^{mdx} + Vehicle group; § p<0.05 vs trial 1 of the same group (Friedman test followed by Dunn's post hoc test).

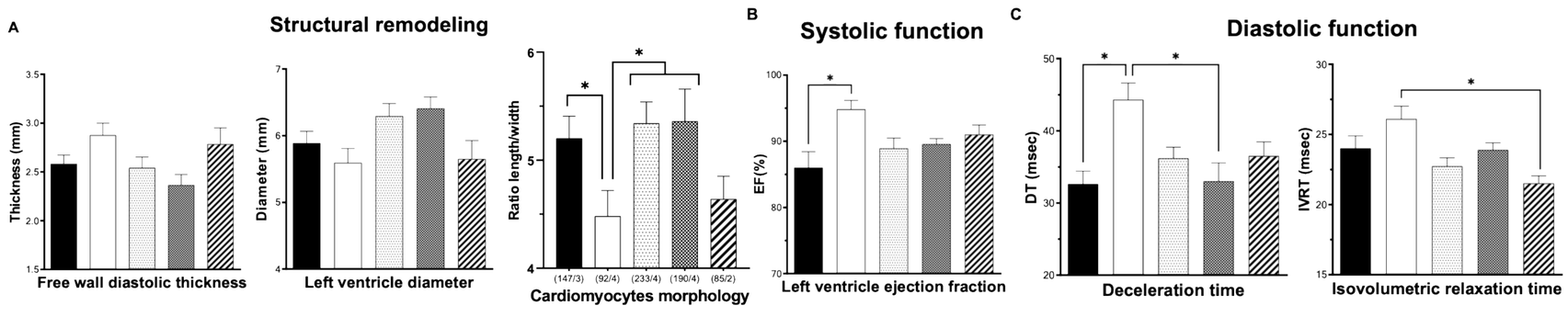

Figure 8: Analysis of cardiac function in DMD^{mdx} rats injected with rAAV2/9-MD1 and rAAV2/9-MD3 vectors.
(A): Structural remodeling of the heart: free wall diastolic thickness and left ventricle diameter were assessed by Two-dimensional (2-D) echocardiography in the different experimental groups at 3 months post-injection (N=11 animals for the DMD^{mdx} + MD1 3E13 group; N=9 animals for the DMD^{mdx} + MD1 1E13 group; N=10 animals for the other group). Cardiomyocytes morphology was assessed by the measuring length/width ratio of isolated cardiomyocytes obtained at sacrifice. Data are presented as mean ± SEM from n cardiomyocytes and N animals. * p<0.05 (ANOVA test, followed by post-hoc Bonferroni multiple comparison test). Systolic (B) and diastolic (C) functions of the heart: left ventricular ejection fraction, deceleration time and isovolumetric relaxation time was assessed by pulsed Doppler in the different experimental groups at 3 months post-injection (N=11 animals for the DMD^{mdx} + MD1 3E13 group; N=9 animals for the DMD^{mdx} + MD1 1E13 group; N=10 animals for the other group). Data are presented as mean ± SEM. *p<0.05 (Nonparametric Kruskal-Wallis test, followed by a post-hoc Dunn's multiple comparison test).

→ INCLUSION OF THE CT DOMAIN DOES NOT IMPROVE MD1 THERAPEUTIC EFFICACY ON DMD MUSCULAR AND CARDIAC PATHOLOGIES OF DMD^{MDX} RATS

Conclusions

Taken together, our results indicate that the inclusion of the CT domain does not provide a therapeutic benefit to MD1, at least after 3 months of treatment in DMD^{mdx} rats. Our results indicate indeed that MD1 is able to restore the DAPC at a physiological level. We also confirmed in a relevant model of DMD that systemic administration of a rAAV-MD1 vector at 3E13 vg/kg significantly improved histological pattern, muscle force and DMD-related cardiac pathology. We also showed for the first time that MD1 significantly improves DMD-related calcium homeostasis alterations in skeletal muscles and heart. Alltogether, our results strengthened the evidence of the therapeutic efficacy of MD1.

UMR 1089 Translational Gene Therapy for Genetic Diseases · The Ohio State University Campus Chemical Instrument Center · Therassay Preclinical Therapeutic Assay · l'institut du thorax · APEX · Trip Transgenese Rat et ImmunoPhenomique · Royal Holloway University of London · UCL Great Ormond Street Institute of Child Health · Oniris · Université de Nantes · Centre Hospitalier Universitaire de Nantes · Inserm · AFM Telethon · MDA For Strength, Independence & Life · Fondation d'Entreprise Hérapie Génio